EFFECT OF MICROSTRUCTURE ON FATIGUE IN NEAR THRESHOLD REGION IN V/Nb DUAL PHASE STEEL

K.Gerić* and D. Drobnjak**

Propagation of long fatigue cracks in the near threshold region has been investigated in a V/Nb ferritic-martensitic steel heat treated to produce a range of dual-phase microstructures. The propagation threshold, ΔK_{th}, is found to increase with increasing strength level, volume fraction and connectivity of martensite. For sample containing 5 to 10% martensite, which corresponds to a yield strength of 320 MPa, the threshold was 10 MPa $\sqrt{m}$; whereas for 70 to 75% martensite, yield strength 700 MPa, the threshold was 18 MPa $\sqrt{m}$. SEM studies showed that whilst cracks run predominantly through the ferrite phase in low martensite samples and through the martensite in high martensite samples, ferrite/ferrite and ferrite/martensite interfaces often serve as preferred paths.

INTRODUCTION

It is well known that some duplex ferritic/martensitic microstructures give rise to superior fatigue crack growth thresholds in long cracks (1) to (5). However, the role of martensite in the near threshold region is not well understood. For example, there has been no systematic investigation of the effect of the volume fraction of martensite on the fatigue threshold. Whereas some results show that a large volume fraction of ferrite is important for achieving high thresholds combined with high strength, more recent work contradicts this (5). Other workers have reported that the fatigue threshold is unaffected by the volume fraction of martensite (3), (4).

The aim on this work was to determine the effect of the volume fraction of martensite on the crack propagation threshold. Different heat treatments were used to vary the proportion, morphology and distribution of martensite.

* Faculty of Mechanical Engineering, Novi Sad, Yugoslavia.
** Faculty of Technology and Metallurgy, Belgrade, Yugoslavia.

EXPERIMENTAL PROCEDURE

Material and Heat Treatment. The material used in this study had a composition (in wt.pct.) of 0.083 C, 1.44 Mn, 0.33 Si, 0.039 Al, 0.045 Nb and 0.072 V. In order to develop a range of duplex microstructures, the heat treating procedures, given in figure 1, were followed.

Fatigue Testing. Specimens, 7.5 mm thick, 20 mm wide and 90 mm long were machined from the as-received 8 mm thick hot rolled sheet. Three point bend specimens with a 1.5 mm deep notch were used for crack propagation studies. After machining the notch, the fatigue specimens were polished, and then a set of parallel lines traced on the polished surface at 0.5 mm intervals from the notch tip.

The fatigue tests were carried out on a 20 kN Amsler testing machine. All tests were run under load control at a frequency of 80 Hz, with $P_{min}/P_{max} = 0.2$.

For the determination of the threshold stress intensity range, ΔK_{th}, a stepwise ΔK-decreasing test was used (1), (2). The crack was initially grown 1 mm from the notch tip, and the load was then in 10% decrements. Between load decrements the crack was allowed to grow 0.5 mm. This procedure was followed until a stress intensity range was reached at which no growth was detected in 10^6 cycles. This stress intensity range was defined as the threshold level, ΔK_{th}.

SEM Investigation. Scanning electron metallography and fractography were used to study the propagation path and fracture surface respectively.

Quantitative metallographic techniques were employed to determine the ferrite grain size, the volume fraction of martensite and the degree of connectivity of the martensite structure.

Following reference (1) the connectivity of the martensite structure is defined by the parameter $\Psi = N_g/(N_g + N_b)$, where N_g is the average number of intersections with boundaries of the martensitic structure per unit of length (mm^{-1}) and N_b is the average number of intersections with the grain boundaries of the ferrite per unit length, excluding the length shared by the martensitic structure (mm^{-1}).

RESULTS

Microstructure and Tensile Properties. Three types of microstructures were developed in dual-phase steel; one consisted of islands of martensite at ferrite grain boundaries (figure 1a,1b,1c,1g,1k), the second consisted of a contineous martensitic network (figure 1e,1f,1j) and the third consisted of islands of ferrite within a martensitic matrix (figure 1d,1h,1i). Irrespective of the heat treatment used (HTSQ, DQ, LTSQ) the intercritical temperature and the cooling rate from the intercritical range determine the amount of martensite and martensite connectivity. The relevant results are summarised in table 1 together with the tensile data and the fatigue threshold properties. The data in table 1 show that the volume fraction of martensite and the martensite connectivity correspond nearly one- to -one. The tensile properties, notably the yield and ultimate tensile strength, reveal that several grades of dual-phase steels are produced, depending on the volume fraction of martensite. They range from typical high formability steels (with a low yield strength of 320 to 360 MPa, and a high ultimate tensile strength of 620 to 660 MPa) up to high yield strength steels (700 to 730 MPa)

Fatigue Crack Propagation Threshold. The results of table 1 show that irrespective of the volume fraction of martensite and the martensite connectivity, the threshold is generally well above 10 MPa √m. It should also be noted that a high threshold level of the order of 18 to 20 MPa √m is obtained in some specimens, notably those with a high volume fraction of martensite and a high martensite connectivity. To illustrate this effect better, the data of table 1 are plotted in figures 2 and 3 to show that ΔK_{th} increases with both the volume fraction and the connectivity of the martensite. In addition, the threshold as a function of yield and ultimate tensile strength is shown in figure 4 and 5 respectively. Again the threshold increases both with increasing yield and ultimate tensile strength.

Crack Path and Fracture Surface. Scanning electron micrographs of polished and etched sections containing cracks revealed (figure 6) that both transgranular (through ferrite and martensite) and intergranular (along ferrite/martensite and ferrite/ferrite interfaces) modes of fracture occur in the near-threshold region of the dual-phase steels studied in this work. At a small volume fraction of ferrite the crack propagates predominantly through ferrite (figure 6a), at somewhat larger volume fractions through both ferrite and martensite (figure 6b), and at a still larger volume fractions predominantly through martensite (figures 6c and 6d). However, propagation along ferrite/ferrite and ferrite/martensite interfaces (denoted by arrows in figures 6b, 6c and 6d) is frequently observed. There are no obvious differences in the crack path between various microstructures. Deviation from the plane of maximum tensile stress leading to a tortuous crack path is exhited by all microstructures studied in this work (figure 6).

Scanning electron fractographs of fracture surface, in addition to the "hill-and-wally" appearance commonly associated with the transgranular mode of fracture (figure 7a), reveal intergranular fracture (denoted by arrow in figure 7b) and shear facets in both low (denoted by SF in figure 7b) and high (denoted by SF in figure 7c) martensitic structures.

DISCUSSION

The focus of this investigation was the role of the martensite on the near-threshold fatigue crack growth in duplex ferrite/martensite structures. For this reason the volume fraction of martensite was changed whilst maintaining a roughly constant ferrite grain size (table 1)

The lowest treshold level,of the order of 10 MPa $\sqrt{m}$ (table 1) in the present investigation, is associated with a duplex structure (figure 1a) comprising a high volume fraction of ferrite (90 to 95%). This value is very close to the threshold values encountered in low carbon ferrite steels (6) to (8), thus indicating that martensite, when present in small fractions, has little if any effect on the fatigue crack propagation in the near threshold region of duplex steels. However, at a larger volume fraction, i.e. in excess of 15% (figure 2), martensite may play an important role, which seems to be contrary to some previous findings (1) to (4). For instance, according to McEvily and co-workers (1) to (2), a large volume fraction of ferrite in addition to a high degree of martensite connectivity is important for achieving high thresholds. However, some recent results by the present authors (5) seem to contradict this proposition. Moreover, recent studies by Wasynczuk et al. (3) and Dutta et al. (4) show that the threshold values are unaffected by changing the volume fraction of martensite from 35 to 48% and from 32 to 58%, respectively (in Suzuki's and McEvily's work (1) martensite was varied from 50 to 65%). A common factor in all these studies is a relatively narrow range of martensite content (35 to 65%). If the same range was selected in the present study, then the results would be equally inconclusive, but when the entire range (5 to 80%) is considered (figure 2) then in spite of considerable scatter, an increase in the threshold level with increasing volume fraction of martensite, seems to be reasonably well established. However, the present results indicate that the treshold level may equally well be related to the degree of martensite connectivity (figure 3). A high martensite connectivity together with a high volume fraction of ferrite is reported to be responsible for high thresholds (1), (2). In this connection, it is assumed (1), (2) that plastic deformation of the ferritic grains is constrained by the surrounding hard martensite phase, thus promoting a higher closure level, but only in the presence of a high fraction of ferrite. However, the present results, as well as previous results by the same authors (5), show that neither a large martensite connectivity nor a high fraction of ferrite is necessary in many cases (table 1). This indicates that the plastic constraint closure mechanism is not likely to be operative in the present case. Still the fact remains that high threshold values are generally associated with high closure levels, as revealed by direct measurement of the closure level (4) and expected from the shear-mode crack growth (1) to (5) and tortuous crack path (2) to (4). To account for these observations a roughness-induced crack closure mechanism is suggested (3) and (4) to be operative, together with a crack deflection mechanism (4), (9). However, the present results, while somewhat inconclusive in respect to the overall roughness of the fracture surface, clearly show that a tortuous crack path (figure 6) and shear mode of fracture (figure 7) is associated not only with microstructures exhibiting a high (figures 6d and 7c) but also a low threshold levels (figures 6a and 7b). Therefore, it seems reasonable to assume that in the present case besides the roughness induced crack closure and the crack deflection, some additional mechanisms are likely to operate. For instance the residual stresses which are introduced into duplex structure during the austenite/martensite transformation (10) may play an important role. These, presumably compressive stresses which are predominantly located in the ferrite next to the ferrite/martensite interfaces (10), may change the stress pattern at the crack tip, and stop the fatigue crack growth. If this mechanism was operative, then the increase in the threshold level with increasing volume fraction of martensite observed in this work, may at least in part be attributed to the increased residual stress level. Since the stability of the residual stresses depend on the relaxation ability of the ferrite, the role of ferrite/martensite volume fraction may easily be understood. However, the contribution from the residual stresses in comparison to the crack closure and deflection mechanisms is difficult to estimate, since the level of residual stresses is also strongly dependent on factors such as steel composition, heat treatment conditions and grain size.

SUMMARY

The fatigue crack propagation threshold ΔK_{th}, increases with increasing strength level, martensite connectivity and volume fraction of martensite, which coexists with ferrite in the dual-phase steels studied in this work. A threshold level of about 10 MPa $\sqrt{m}$ is encountered in samples comprising 5 to 10% martensite, corresponding to a yield strength of about 320 MPa. For 70 to 75% martensite (yield stress 700 MPa) the threshold was 18 MPa $\sqrt{m}$. Scanning electron metallography and fractography investigations have shown that martensite affects the fatigue crack path in such

a way that, whilst cracks run predominantly through ferrite in low martensite samples and through martensite in high martensite samples, martensite/ferrite interfaces are often followed as a preferred path.

In addition, a tortuous crack path and the shear mode of fracture is associated not only with microstructures exhibiting a high but also low threshold level. The superior near-threshold fatigue resistance of dual phase steels containing a high volume fraction of martensite is proposed to be, at least in part, due to the residual stresses introduced into the ferrite during martensite formation; this effect probably operating together with the crack closure and the crack deflection effects suggested previously (1) to (4).

REFERENCES

(1) Suzuki, H. and McEvily, A.J., Metall. Trans. A, Vol. 10A, 1979, pp. 475-481.

(2) Minakawa, K., Matsuo, Y. and McEvily, A.J., Metall. Trans., A, Vol. 13A, 1982, pp. 439-445.

(3) Wasynczuk, J.A., Ritchie, R.O. and Tomas, G., Mater. Sci. Eng., Vol. 62, 1984, pp. 79-83.

(4) Dutta, V.B., Suresh, S. and Ritchie, R.O., Metall. Trans. A, Vol. 15A, 1984, pp. 1193-1207.

(5) Gerić, K. and Drobnjak, D., ECF5, Lisbon, 1984, pp. 115-123.

(6) Beevers, C.J., Metal. Science, Vol. 14, 1980, pp. 418-423.

(7) Paris, P.C., et al., Stress Analysis and Growth of Cracks, ASTM STP 513, 1972, pp. 141-176.

(8) Pook, L.P., Stress Analysis and Growth of Cracks, ASTM STP 513, 1972, pp. 106-124.

(9) Suresh, S., Metall. Trans., A, Vol. 14A, 1983, pp. 2375-2385.

(10) Moyer, J.M. and Ansell, G.S., Metall. Trans., A, Vol. 6A, 1975, pp. 525-530.

TABLE 1 - Structure, Tensile and Fatigue Properties of V/Nb Dual-Phase Steel

Nº	Heat Treatment x)	Mart. Vol. Fract. (pct)	Mart. Conn. (pct)	Ferr. Grain. Size (um)	UTS (MPa)	$\sigma_{0.2\%}$ (MPa)	Elong (pct)	K_{th} (MPa$\sqrt{m}$) Single measurement			K_{th} (MPa$\sqrt{m}$) Average
1.	HTSQ (k)	5	5	10	553	348	25.5	10.8	10.7		10.8
2.	DQ (g)	10	10	7	618	321	22.5	10.9	9.1	8.6	9.6
3.	LTSQ (b)	15	20	7	655	340	18.0	14.9	14.6		14.7
4.	LTSQ (a)	15	20	5	663	363	22.5	9.2	10.9		10.1
5.	LTSQ (c)	20	30	9	693	390	20.5	12.8	13.0	12.7	12.8
6.	DQ (f)	30	50	9	826	484	17.0	14.8	17.1		15.9
7.	DQ (e)	40	60	8	920	547	17.5	13.2	13.2		13.2
8.	HTSQ (j)	60	70	5	911	619	15.3	13.9	12.0		13.0
9.	DQ (d)	70	70	4	995	728	12.5	16.9	19.8		18.3
10.	HTSQ (h)	75	90	3	976	706	15.0	15.9	20.2		18.0
11.	HTSQ (i)	80	90	4	1021	728	15.0	13.5	14.4		14.0

x) Refer to Figure 1

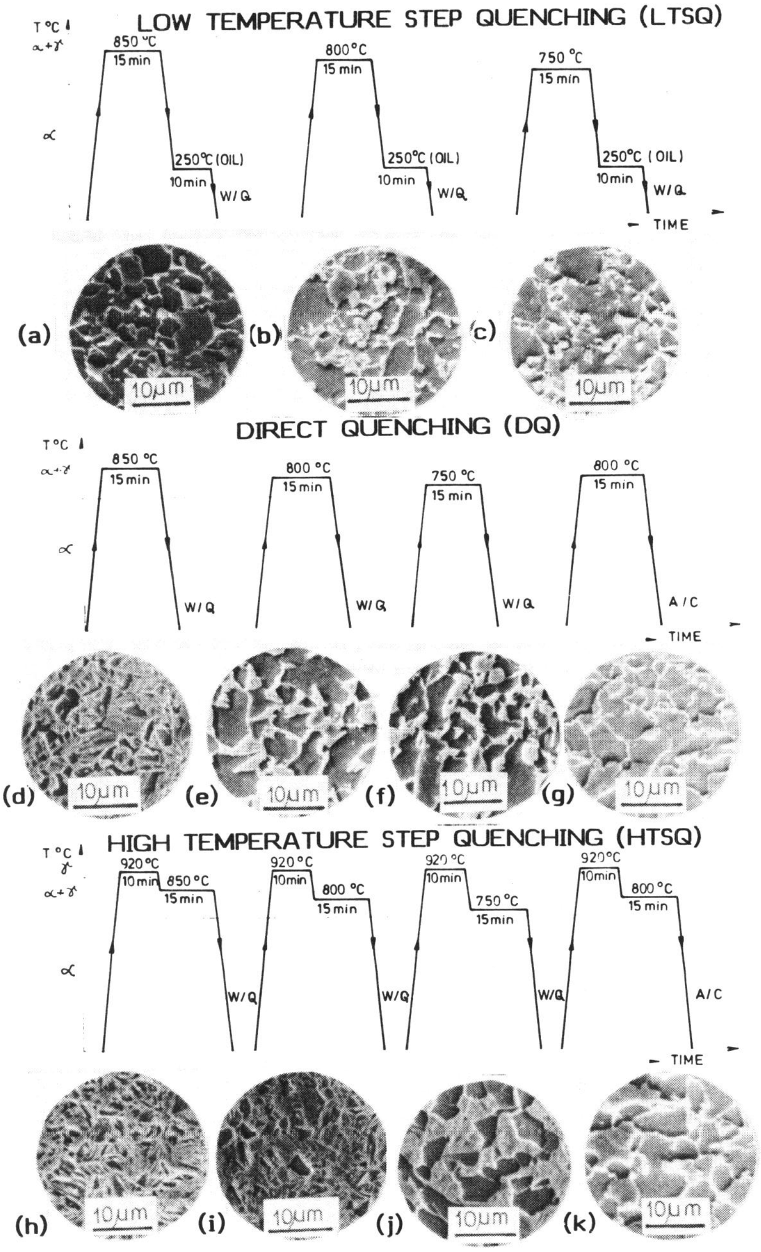

Figure 1 Heat treatment cycles and resulting duplex microstructures (W/Q - water quenching; A/C - air cooling).

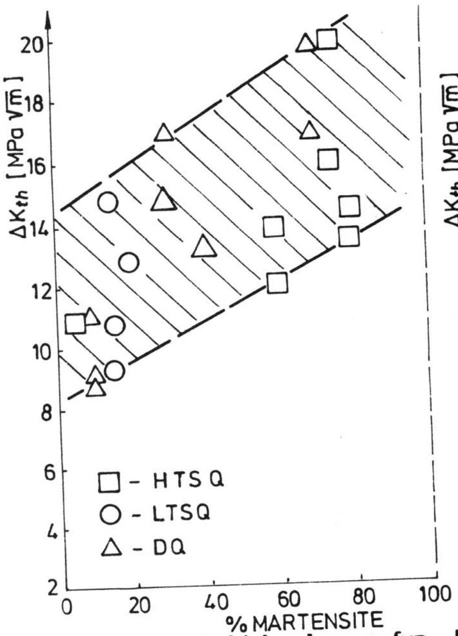

Figure 2 Threshold level as a function of a volume fraction of martensite

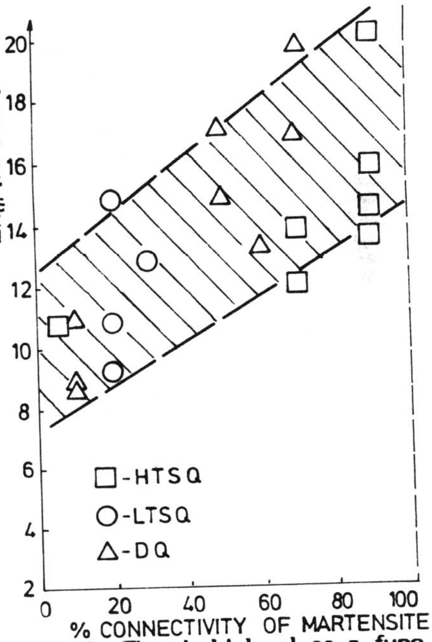

Figure 3 Threshold level as a function of connectivity of martensite

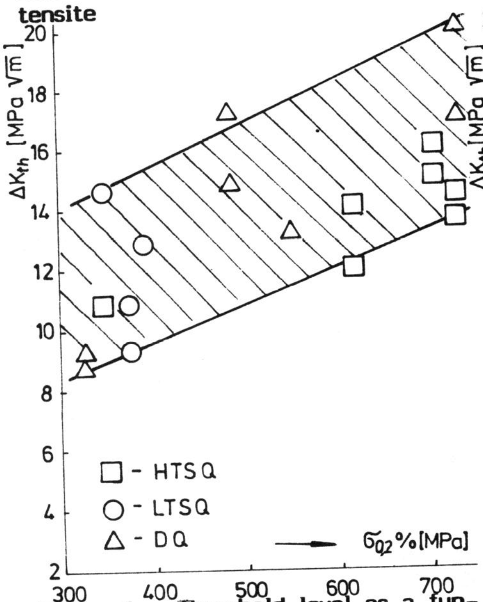

Figure 4 Threshold level as a function of yield strength

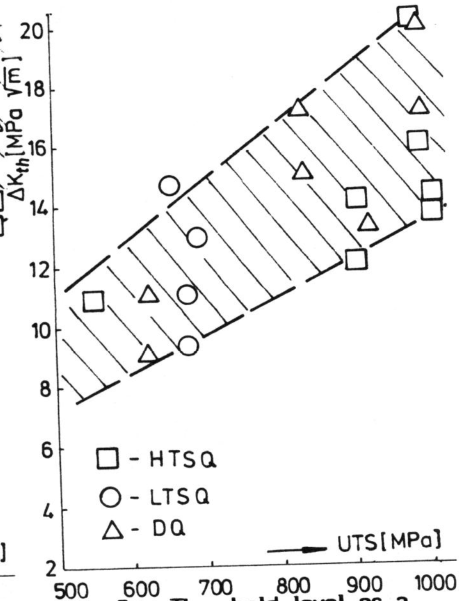

Figure 5 Threshold level as a function of ultimate tensile strength.

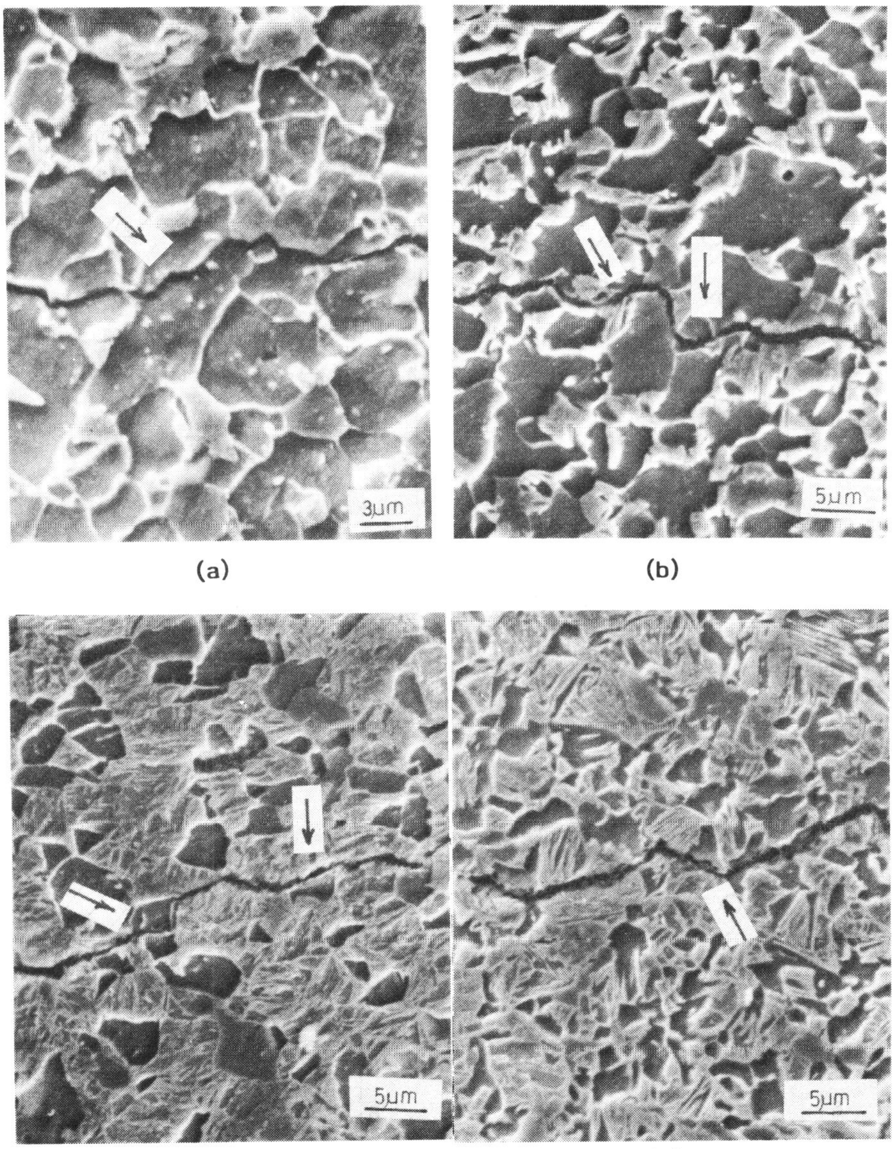

Figure 6 Scanning electron micrographs of crack path at near threshold level (a) air cooling from 800°C (b) direct quenching from 750°C (c) higrh temperature step quenching from 920/750°C (d) direct quenching from 850°C.

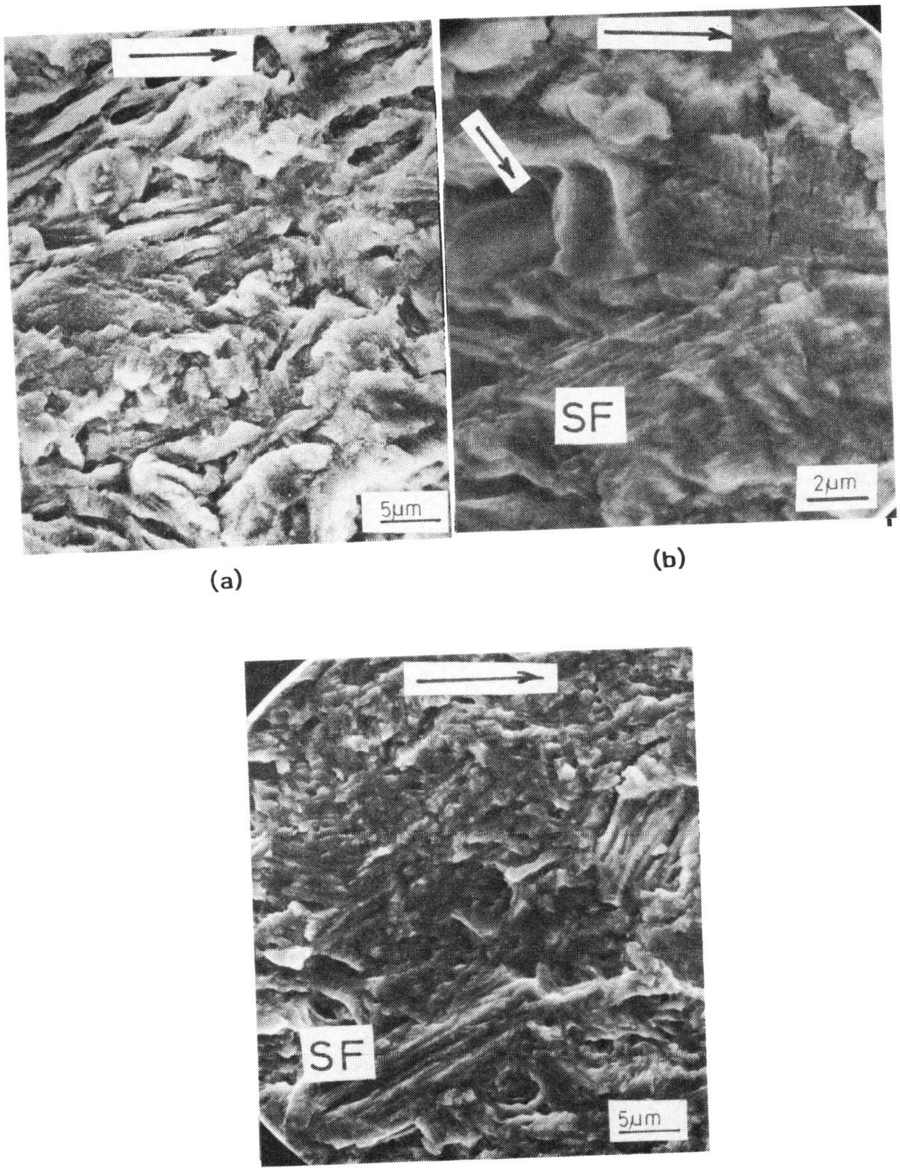

(a) (b)

(c)

Figure 7 Scanning electron fractograph of fatigue fracture surfaces at near threshold level (a) air cooling from 800°C (b) high temperature air cooling from 920/800°C (c) high temperature step quenching from 920/800°C.